

Image Restoration in Dual Energy Digital Radiography using Wiener Filtering Method

Byoung-Goo Min, Kwang-Suk Park

= Abstract =

Wiener filtering method was applied to the dual energy imaging procedure in digital radiography(D.R.). A linear scanning photodiode arrays with 1024 elements(0.6mm×1.3mm pixel size) were used to obtain chest images in 0.7 sec. For high energy image acquisition, X-ray tube was set at 140KVp, 100mA with a rare-earth phosphor screen. Low energy image was obtained with X-ray tube setting at 70KVp, 150mA.

These measured dual energy images are represented in the vector matrix notation as a linear discrete model including the additive random noise. Then, the object images are restored in the minimum mean square error sense using Wiener filtering method in the transformed domain. These restored high and low energy images are used for computation of the basis image decomposition. Then the basis images are linearly combined to produce bone or tissue selective images. Using this process, we could improve the signal to noise ratio characteristics in the material selective images.

1. Introduction

Dual energy imaging method proposed by Alvarez and Macovski has been applied in digital radiographic system by several authors (Lehman 1981 ; Brody 1981 ; Takeuchi 1986). Most of them are concerned with methods and techniques which can increase the seperability of basic materials(bone and tissue) and simplify the seperation modality(Wong 1983 ; Brody 1984). However, these improved seperation characteristics were obtained with increased

image noise, thus it results in the reduction of SNR in the final images.

There are many kinds of noise sources which can deteriorate image qualities, such as 60Hz X-ray ripple, quantum noise, image blurring due to scattered radiations, image degradation due to the motion of the detector assembly, and image blurring generated in X-ray to light conversion process. Some of these can be calibrated or eliminated by the improved hardware performances and accuracies. However the remaining systematic noises and blurrings can be accentuated in the dual energy computation.

We applied the Wiener filtering method for each images of high and low energy before computation of basis images to minimize the

<접수 : 1987년 12월 15일>

Dept. of Biomedical Eng., Seoul National University

* 본 연구는 1986년도 서울대학교병원 임상 연구비 보조에 의한 것임.

SNR deterioration in the bone and tissue selective images.

2. Materials and methods

The dual energy images with Wiener filtering method is obtained in the following five steps as illustrated in Fig. 1. First, calibration images and chest phantom images are obtained with high and low X-ray photon energies separately. Second, these high and low energy images are processed using Wiener filter respectively. Wiener filter parameters and additive noise characteristics are obtained by test procedures. Third, calibration images are used for the estimation of model coefficients and these coefficients are used for the estimation of basis images. Fourth, after determination of basis images, material selecting

angles are estimated with variation of combination. Fifth and finally, material selective images are estimated as a linear combination of basis images with the above estimated angles. The details are described in the following sections.

2-1. Wiener filtering

Among the noise components in the system, some noises such as quantum noise, blurring due to scattered radiations and screen characteristics, and blurring caused by the motion of the detector assembly, can be characterized by the test procedures and can be used for the restoration of images. Wiener filtering method is optimal in the mean square error sense under the known system and noise characteristics.

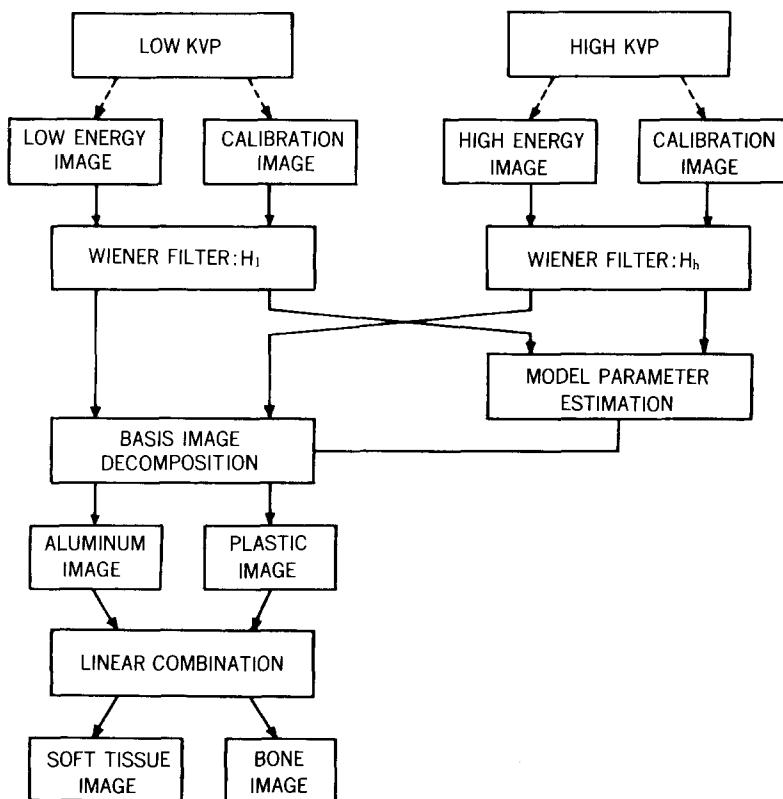


Fig. 1. Dual energy technique with Wiener filtering method

We represent images using a linear model as follows.

$$g_l(x, y) = f_l(x, y) * h_l(x, y) + n_l(x, y) \quad (1)$$

$$g_h(x, y) = f_h(x, y) * h_h(x, y) + n_h(x, y) \quad (2)$$

where $g_i(x, y)$: image obtained using experimental system

$h_i(x, y)$: point spread function of the system

$n_i(x, y)$: additive, zero mean, independent random noise representing system noises

$f_i(x, y)$: original image
(i=1 for low energy image
i=h for high energy image)

Above model can be represented by vector matrix notation.

$$g_l = H_l \cdot f_l + n_l \quad (3)$$

$$g_h = H_h \cdot f_h + n_h \quad (4)$$

g_i, f_i, n_i are column stacked $N^2 \times 1$ vectors of $g_i(x, y), f_i(x, y), n_i(x, y)$ respectively, and H_l, H_h are $N^2 \times N^2$ block Toeplitz point spread function matrices. Restored images f_l, f_h can be calculated by Wiener filtering method.

$$f_l = K_{ll} H_l (H_l K_{ll} H_l + K_{nl})^{-1} g_l \quad (5)$$

$$f_h = K_{hh} H_h (H_h K_{hh} H_h + K_{nh})^{-1} g_h \quad (6)$$

$K_{ll}, K_{lh}, K_{nl}, K_{nh}$ are the autocorrelation functions of images and noises obtained at low and high energies. For stationary system, the autocorrelation matrix is in block Toeplitz form, and can be approximated to circulant form. And, these circular matrices are diagonalized by the Fourier transform and Wiener filter can be evaluated in transformed domain.

$$F_l(u, v) = \frac{S_{nl} H_l^*(u, v) G_l(u, v)}{S_{ll}(u, v) |H_l(u, v)|^2 + S_{nl}(u, v)} \quad (7)$$

$$F_h(u, v) = \frac{S_{nh}(u, v) H_h^*(u, v) G_h(u, v)}{S_{hh}(u, v) |H_h(u, v)|^2 + S_{nh}(u, v)} \quad (8)$$

where S_{li}, S_{ni} : power spectral densities of signal noise respectively.

$F_i(u, v), G_i(u, v), H_i(u, v)$: Fourier transforms of f_i, g_i, h_i

(i=1 for low energy image

i=h for high energy image)

H_l and H_h are estimated by curve fitting of the measured point spread function to Gaussian shape function. S_{nl} and S_{nh} are estimated from test scanning without any object.

Fourier transforms of processed images are evaluated by inverse Fourier transforms. Estimated images are applied to the next procedure of the basis image decomposition and the linear combination for the selective imaging.

2-2. Calibration procedures

The purpose of calibration procedure is to obtain the coefficients required for estimation of equivalent thicknesses of the basis materials. An aluminium step wedge with eight steps of 0.2cm thicknesses and a plastic step wedge with 17 steps each of 0.5cm thickness were used for calibration. These step wedges are stacked across so that all possible combinations of material thicknesses can be obtained in a single scan. Kodak Lanex rare earth screen was used for high energy(140KVp, 50mA) image acquisition to increase the separability of energy spectra, and low energy image was obtained at 70KVp(100mA). Then, logarithmic values of pixels were used for estimation of coefficients.

We used the polynomial function of equation (9) and (10) to estimate the basis images of the aluminium($A(x, y)$) and plastic($P(x, y)$) from high and low energy images ($f_l(x, y), f_h(x, y)$) as follows.

$$A(x, y) = A0 + A1 Dl(x, y) + A2 Dh(x, y) + A3 Dl(x, y)^2 + A4 Dh(x, y)^2 + A5 Dl(x, y) Dh(x, y) + A6 Dl(x, y)/Dh(x, y) + A7 Dh(x, y)/Dl(x, y) + A8 Dl^3(x, y) + A9 Dh^3(x, y) \quad (9)$$

$$P(x, y) = P0 + P1 Dl(x, y) + P2 Dh(x, y) + P3 Dl(x, y)^2 + P4 Dh(x, y)^2 + P5 Dl(x, y) Dh(x, y) + P6 Dl(x, Y)/Dh(x, y) + P7 Dh(x, y)/Di(x, y) + P8 Dl^3(x, y) + P9 Dh^3(x, y) \quad (10)$$

where $DI(x, y) = \log(I_0/f(x, y))$

$Dh(x, y) = \log(I_0/f_h(x, y))$

Calibration data and known aluminium and plastic thickness are used to estimated coefficients A_i and P_i (for $i=0, \dots, 9$) for the experimental system. To determine coefficients in the least-square error sense, Gaussian elimination technique was used.

2-3. Linear calibration

After determining the basis images with the estimated coefficients, we can selectively enhance the images corresponding to the material of interest, such as bone or soft tissue by proper combination of these basis images at a specific angle in the domain of aluminum and plastic components. With selective anagle, θ , the material selective components is calculated at each pixel as follows.

$$C(x, y) = A(x, y) \sin\theta + P(x, y) \cos\theta \quad (11)$$

This linear combination is computed with the angle variation, and the best angle is selected for the specific material.

2-4. Experiments

To verify the Wiener filtering method in dual energy techniques, the chest phantom experiments were performed. Fig. 2. shows the block diagram of our own developed experimental D. R. system.

It produces a full field digital image of 1024 by 1024 pixel size, with grey values ranging 0~255. The photodiode detector assembly moves a distance of 66cm during 0.7 sec of scanning time and samples are taken with 0.65mm increments. The detector assembly consists of 1024 photodiode elements.

In this study, a stacked sliced chest phantom was used, and the X-ray potential was set to 70 KVp(150mA) for low energy scan and 140 KVp(100mA) for high energy scan. A Kodak Lanex regular screen was placed in the incident beam for the high energy scan to selectively attenuate the low energy spectra including tungsten characteristics. The raw data from detectors are stored in the memory of digital radiographic system. And, the sub-

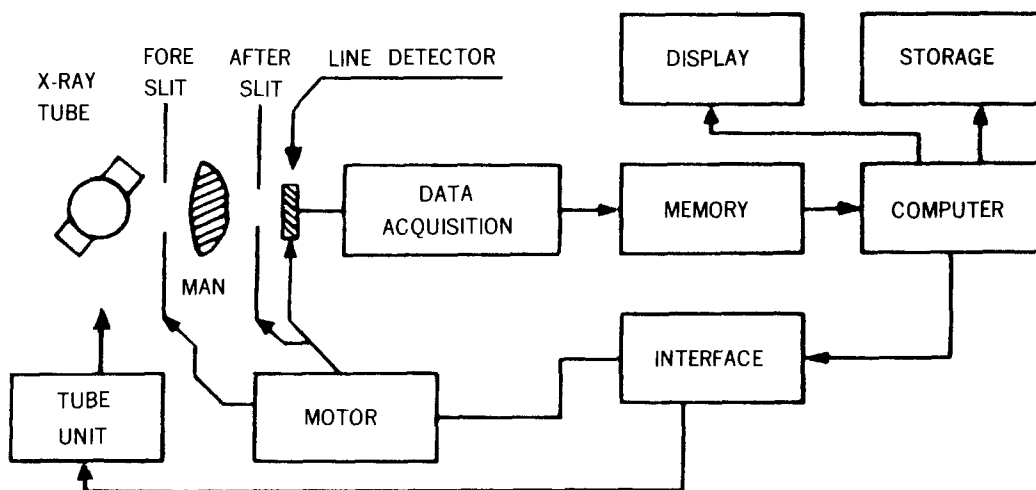


Fig. 2. Block diagram of the SNUH-100 D. R. system

sequent numerical calculations for Wiener filtering, the basis image decomposition and the linear combination are performed with the interfaced IBM PC/AT computer. Finally, the estimated selective images for bone and tissue are displayed on a high resolution monitor(1024 × 1024 resolution).

3. Results

The coefficients for the evaluation of basis images are estimated using the measured calibration data, and summarized in Table 1.

Table 1. Estimated coefficients for basis image decomposition

i	A _i	P _i
0	-1.9	1.2
1	-17.0	5.4
2	30.6	-4.1
3	-13.2	9.0
4	-9.0	-3.2
5	26.0	-11.5
6	1.8	0.4
7	0.7	0.7
8	1.1	-1.0
9	-3.7	3.7

Table 2 shows the measured angles for tissue and bone selective images of chest phantom. Bone selective image is nearly equivalent to the aluminium basis image, and tissue selective image is obtained with the rotation angle of 5 degree.

Fig. 3 shows the measured low and high energy images, the computed tissue selective and bone selective images of the stacked sliced chest phantom. Horizontal strip patterns are due to the surface coating material between each of the stacked phantom slices.

Fig. 4 shows the tissue selective image and bone selective images, respectively, after the Wiener filtering method. The calculated local

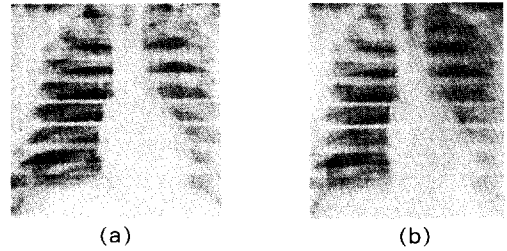


Fig. 3. Stacked sliced chest images by dual energy techniques : low energy image (a), high energy image (b)

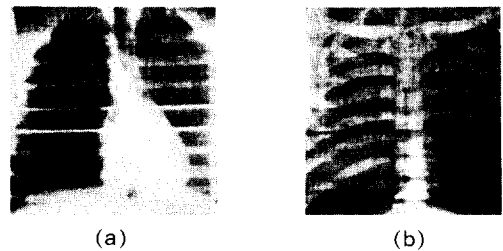


Fig. 4. Selective images with Wiener filtering method : tissue selective image (a), bone selective image (b)

SNR was improved by 25% to 46% in the final images after Wiener filtering method.

Table 2. Measured angles of selected materials

	Measured angle(degree)
Plastic	0
Aluminum	90
Tissue	5
Bone	90

4. Discussion and conclusion

In this procedure, Wiener filter was applied before the basis image decomposition. In the dual energy technique, noise characteristics are more deteriorated in decomposed basis images and material selective images due to the amplification effects in the dual energy techniques. Thus it is more preferable to use

Wiener filtering after basis image estimation than prior to basis image computation. However, the estimation of Wiener filter parameters is difficult in this case due to the non-linearity in the process of basis image decomposition. We are now studying the use of second high performance sensor in the selected small area for estimation of Wiener filter parameters, and then it may be possible to apply Wiener filter after basis image decomposition with improved performance.

Since two separate scans are necessary for low and high energy images, any motion or misregistration between two images can produce significant motion blurring effects. These effects can further deteriorate SNR characteristics in the final material selective images. Thus in the clinical system, it is desirable to obtain the dual energy data in a single scan to eliminate the above problems.

Also the X ray fluctuations in the linear scanning system can cause a significant deterioration in image quality. Even in the present digital radiographic system with three phases generator and hardware compensations, there still remains residual fluctuation effects, which were amplified in the material selective

images.

In conclusion, the high SNR characteristic is much more significant in dual energy digital radiographic system due to amplification effects in the computation procedure. Thus, Wiener filtering procedure is desirable to improve image quality in dual energy technique.

References

- 1) Brody WR, et al. *Dual-Energy Projection Radiography: Initial Clinical Experience.* *AJR* 1981, 137; 201~205.
- 2) Brody WR. *Digital Radiography.* Raven Press. 1984.
- 3) Lehman LA, Alvarez RE, Macovski A, Brody WR. *Generalized image combinations in dual K Vp digital radiography.* *Med. Phys.* 1981, 8; 659~667.
- 4) Takeuchi H, Chuang K, Huang HK, *Dual-Energy Imaging in Projection Radiography.* *SPIE.* 1986, 626; 30~48.
- 5) Wong CK. *Calibration procedure in dualenergy scanning using the basis function technique.* *Med. phy.* 1983, 10; 628~635.
- 6) 민병구, 박광석 외. 디지털 X-선 시스템에 관한 연구. *의공학회지.* 1986, 7~1; 45~51.

국문 초록

위너 필터를 이용한 이중에너지 X-선 촬영 영상 복원

민 병 구 · 박 광 석

위너필터의 방법을 디지털 촬영 시스템의 이중에너지 영상 분리방법에 적용하여 잡음의 영향을 줄였다. 실험에 사용된 시스템은 선형 검출기를 기계적으로 구동하여 0.7초내에 수집한다. 선형 검출기는 1024개의 광다이오드 소자들로 구성되어 있고, 각 광다이오드 소자의 수광면적은 1.3mm×0.6mm이다.

고에너지 영상은 발생관의 전압을 140KVp(100mA)로 하여 촬영하였으며, 저에너지의 영상은 70Kvp(150mA)로 하여 촬영하였다. 측정된 영상은 가산 잡음을 포함한 선형 이산 모델로 나타내었으며, 평균 자승 오차가 최소가 되도록 주파수 평면에서 위너 필터를 적용하였다.

이렇게 복원된 영상을 이중에너지를 사용한 기본 물질의 분리와 물질선택적 영상법에 적용하였다.

서울대학교 의과대학 의공학교실